

Electrochemical synthesis, characterization and electro-oxidation of methanol on platinum nanoparticles supported poly(*o*-phenylenediamine) nanotubes

T. Maiyalagan*

Department of Chemistry, School of Science and Humanities, VIT University, Vellore 632014, India

Received 17 January 2008; accepted 22 January 2008

Available online 3 February 2008

Abstract

The electrochemical synthesis and the characterization of Pt nanoparticles dispersed poly(*o*-phenylenediamine) (PoPD) nanotube electrodes, employing alumina membrane as templates are reported. The morphology of the electrodes was characterized by scanning electron microscopy (SEM), atomic force microscopy (AFM) and transmission electron microscopy (TEM). Catalytic activity and stability for the oxidation of methanol were studied by using cyclic voltammetry and chronoamperometry. The results show that poly(*o*-phenylenediamine) nanotubes electrodes significantly enhance the catalytic activity of platinum nanoparticles for oxidation of methanol. The results obtained affirm that the dispersion of the platinum particles is connected with catalytic response to a higher activity. The chronoamperometric response confirms the better activity and stability of the nanotube-based electrode compared to the commercial 20 wt.% Pt/C (E-TEK) and template-free electrode. The nanotubular morphology of poly(*o*-phenylenediamine) helps in the effective dispersion of Pt particles facilitating the easier access of methanol to the catalytic sites. The poly(*o*-phenylenediamine) nanotubes modified with platinum nanoparticles cause a great increase in electroactivity and the electro-catalytic oxidation of methanol.

© 2008 Elsevier B.V. All rights reserved.

Keywords: Methanol oxidation; DMFC; Conducting polymers; Nanostructured materials; Electro-catalyst

1. Introduction

Fuel cells are considered as one of the options for energy conversion by common man in the future. However, in spite of several decades of concerted attempts, this device has not yet evolved as an economically viable, socially acceptable, easily manipulative tool for energy conversion. It is known that there are a variety of barriers in every aspect of this energy conversion device [1–8]. As far as the hardware of a fuel cell is concerned, it essentially consists of three components, namely the two electrodes and the electrolyte. Pt or Pt-based noble metals are employed as electro-catalyst in both the electrodes. It is, therefore natural that there are attempts to reduce the amount of noble metal loading in the electrodes. This can be achieved by suitably dispersing the noble metals on suitable electronically conducting

supports keeping in view the net energy density derivable from such a device with low metal loadings. To decrease the platinum loading and improve both the oxidation rate and electrode stability, considerable efforts have been applied to the study of electrode materials for the direct electrochemical oxidation of methanol [9–17].

Carbon is the most common catalyst support material that conducts electrons (but not protons). It does not contribute to the transport of protons produced in the electro-oxidation reaction. The alternative is to develop a catalyst support that conducts both protons and electrons efficiently [18–20]. Conducting polymers possess both protonic and electronic conductivity. At this juncture, catalytic particles dispersed on the conducting polymers mainly on polypyrrole (PPY) and polyaniline (PANI) have been extensively studied as electrode material for methanol oxidation [21–23]. Among many conducting and electroactive polymers, poly(*o*-phenylenediamine) (PoPD) is of great interest because of its potential use in various fields of technology. Two interesting properties of PoPD, different from those, characteristic

* Tel.: +91 416 2202465; fax: +91 416 2243092.

E-mail address: maiyalagan@gmail.com.

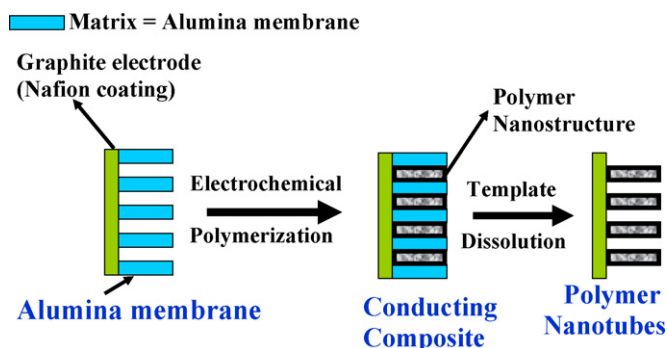


Fig. 1. Template-assisted electrochemical synthesis of conducting polymer nanotube.

for usual conducting polymers like polyaniline or polypyrrole make it promising for applications in electrochemical and bio-electrochemical sensors. One of these properties related to an unusual dependence of the electric conductivity on the redox state of this polymer. As opposed to PANI or PPY, PoPD shows the conductivity in its reduced state, whereas its oxidized state is insulating. This determines the electrochemical properties of PoPD, since many electrode redox processes have been shown to take place within a relatively narrow potential window, corresponding to the reduced (conducting) form of this polymer. Within this potential window, electro-catalytic oxidation of some species proceed, making it possible to use PoPD for electro-catalytic applications, like, e.g. the electro-oxidation of coenzyme NADH, electro-oxidation of methanol [24] and oxygen reduction [25–27].

The detailed synthetic procedures of the poly(*o*-phenylenediamine) nanotube and Pt incorporated template-synthesized poly(*o*-phenylenediamine) nanotube on nafion and graphite are shown schematically in Fig. 1. The conventional synthesis of poly(*o*-phenylenediamine) and Pt deposited poly(*o*-phenylenediamine) nanotube were followed in the same way without the alumina membrane as the template.

The tubular morphology plays a crucial role in the dispersion of the catalytic particles of the conducting poly(*o*-phenylenediamine). In the present investigation, Pt incorporated template-synthesized conducting poly(*o*-phenylenediamine) nanotube has been used as the electrode for methanol oxidation. The composite material based on Pt incorporated template-synthesized poly(*o*-phenylenediamine) has been compared to that of the Pt deposited on conventionally synthesized poly(*o*-phenylenediamine) for electro-oxidation of methanol. These materials are characterized and studied, using scanning electron microscopy (SEM), atomic force microscopy (AFM), transmission electron microscopy (TEM) and cyclic voltammetry.

The electrochemical properties of the nanotube electrode were compared to those of the conventionally synthesized poly(*o*-phenylenediamine) on graphite, using cyclic voltammetry. The Pt incorporated poly(*o*-phenylenediamine) nanotube electrode exhibited excellent catalytic activity and stability compared to the 20 wt.% Pt supported on the Vulcan XC 72R carbon and Pt supported on the conventional poly(*o*-phenylenediamine) electrode. The nanotube electrode showed excellent electro-catalytic activity and stability for electro-oxidation of methanol.

2. Experimental

2.1. Materials

The present work was carried out in aqueous solutions. Purified water obtained by passing distilled water through a milli Q (Millipore) water purification system was used as solvent. *o*-Phenylenediamine (*o*PD) was purchased from Aldrich. Methanol and sulfuric acid were obtained from Fischer chemicals. The alumina template membranes (Anodisc 47) with 200 nm diameter pores were obtained from Whatman Corp. Nafion 5 wt.% solution was obtained from Dupont and was used as received.

2.2. Electrochemical synthesis of polymer nanotubes

All experiments were carried out in a conventional one-compartment cell with a Pt counter electrode and a saturated calomel reference electrode, at room temperature. First the graphite electrode is coated with nafion solution. The nafion not only acts as binder, but also provides both ionic and electronic contact and favours proton transport, and the membrane are hot pressed with the graphite. Secondly graphite electrode was used as a current collector and contact with the template membrane. The membrane together with the current collector was fixed between two Teflon rings. The area of the membrane contacted to the electrode was ca. 1 cm². The solution was de-aerated by bubbling dry nitrogen gas for 5 min before electrochemical polymerization. The electropolymerization of *o*-phenylenediamine was carried out with a BAS 100B Electrochemical Workstation (Bioanalytical Systems Inc., West Lafayette, IN). The poly(*o*-phenylenediamine) nanotubes were grown potentiodynamically from –0.2 to 1.2 V containing 5 mM *o*-phenylenediamine. The length of the nanotube was controlled by the total charges passed in the cell.

2.3. Deposition of Pt particles on graphite/Naf/PoPD_{Temp}

Deposition of platinum particles into the PoPD nanotube by the electroreduction of chloroplatinic acid (0.01 M) in 0.5 M sulfuric acid. Each electro reduction step involved 10 potential cycles in the range from 0.8 to –0.3 V (scan rate = 50 mV s^{–1}).

2.4. Removal of template

The alumina membrane from graphite/Naf/PoPD_{Temp} and graphite/Naf/PoPD_{Temp}–Pt was removed by immersing the composite in 0.1 M NaOH for 15 min. The composite after the dissolution of the template was repeatedly washed with deionized water to remove the residual NaOH. It was subsequently immersed in 1% HBF₄ for 10 min and then washed with deionized water again. The composite after the dissolution of the template was designated as graphite/Naf/PoPD_{Temp} and graphite/Naf/PoPD_{Temp}–Pt. A similar experimental condition was adopted to prepare the template-free Pt incorporated poly(*o*-phenylenediamine) on graphite. The electrode was designated as graphite/Naf/PoPD–Pt. The details of the synthetic

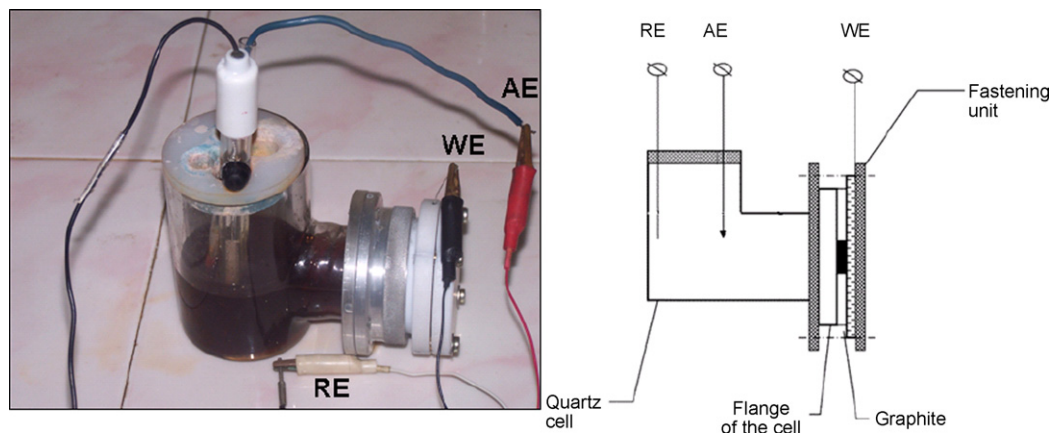


Fig. 2. Schematic view of an electrochemical cell for the formation of nanostructured materials: RE, reference electrode; AE, auxiliary electrode; WE, working electrode (template membrane with a deposited nafion contact layer).

procedure for the preparation of template-synthesized poly(*o*-phenylenediamine) and Pt incorporated template-synthesized poly(*o*-phenylenediamine) are illustrated in Fig. 2.

2.5. Characterization methods

The scanning electron micrographs were obtained using JEOL JSM-840 model, working at 15 keV. The nanorods were sonicated in acetone for 20 min and then were dropped on the cleaned Si substrates. The AFM imaging was performed in air using the Nanoscope IIIA atomic force microscope (Digital Instruments, St. Barbara, CA) operated in contact mode. For transmission electron microscopic studies, the nanorods dispersed in ethanol were placed on the copper grid and the images were obtained using Phillips 420 model, operating at 120 keV.

3. Results and discussion

3.1. Cyclic voltammetry measurements

The electropolymerization of *o*PD monomer on the alumina template was carried out by cyclic voltammetry was shown in Fig. 3. A broad anodic peak appeared in the potential ranged from +0.2 to 1.2 V, which indicated, an oxidative process of *o*PD. In all these cases no reduction peak is found in the reverse scans, thus suggesting that oxidized *o*PD be involved in further chemical processes leading to non-reducible species in the potential range adopted.

3.2. Electron microscopy study

The SEM image of the conventionally synthesized conducting poly(*o*-phenylenediamine) is shown in Fig. 4a. The image shows ladder morphology revealing a dense coverage of poly(*o*-phenylenediamine) on graphite, which are not uniform in nature. Fig. 4b shows the SEM image of the Pt deposited conventionally synthesized poly(*o*-phenylenediamine) on graphite. Though, the Pt crystallites are clearly seen from the image, the cluster size and the geometry of the Pt particles are not uniform and the cluster size was found to be high with agglomerates

as seen over the scanned region. It is further evident from the image that the large Pt crystallites are randomly distributed on poly(*o*-phenylenediamine) and the ladder morphology of the poly(*o*-phenylenediamine) is also seen in the SEM image.

It is evident from Fig. 5a that the uniform, cylindrical, monodisperse nanotubes of PoPD after the removal of the template are projecting perpendicularly to the graphite. The open ends of the uniform nanotube are clearly seen in this image. Fig. 5b shows the picture of the conducting polymeric tubules taken at a tilted angle, in a different region. It is evident from the image that the density of the nanotubes is quite high, in all the regions. These tubes are uniformly distributed in a regular array on the graphite with an outer diameter (200 nm) that almost matches the pore diameter of the template.

AFM image shows the nanotube fibrillar morphology in Fig. 6a representing low magnification. Fig. 6b shows the transmission electron micrograph of Pt incorporated template-synthesized poly(*o*-phenylenediamine) polymer nanotube.

The TEM image does not show visible Pt clusters on the nanotube surfaces. Though the nanotube is clearly seen, the Pt particles are not visible due to the thickness of the wall of the tubules. However, electron diffraction pattern clearly show the

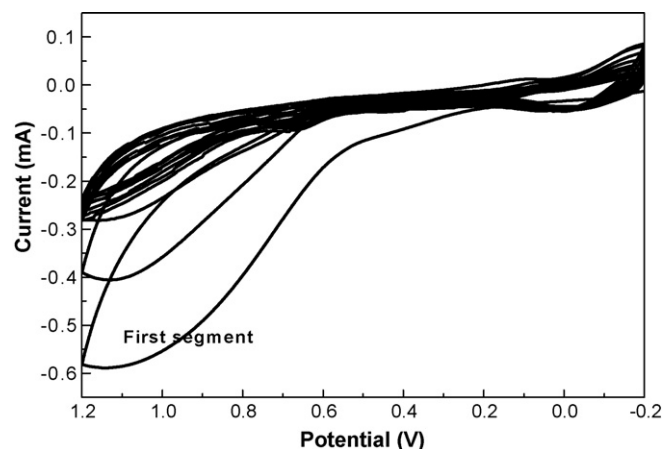


Fig. 3. Cyclic voltammograms obtained during the electropolymerization of *o*-phenylenediamine in 0.5 M *o*PD + 0.5 M H₂SO₄ solution. Scan rate 50 mV s⁻¹.

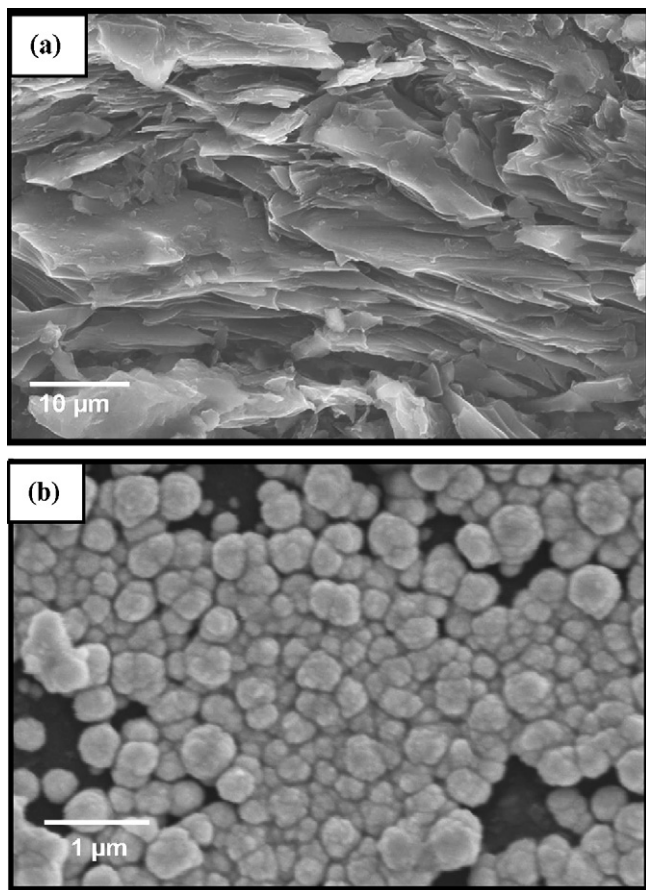


Fig. 4. SEM images of (a) conventionally synthesized PoPD polymer and (b) Pt deposited on conventionally synthesized PoPD polymer.

Pt in the nanotube. The number of concentric rings observed in the electron diffraction image suggests that the Pt particles are finely dispersed in the nanotubules (Fig. 7b). It is suggested that Pt are distributed evenly on both outer and inner surfaces of the nanotubes. The single-crystalline characteristic of several particles is indicated by the presence of lattice fringes (Fig. 7b). The rings correspond to the diffraction from the (1 1 1), (2 0 0), (2 2 0) and (3 1 1) planes of crystalline Pt particles. The observed reflections agree perfectly with those of face-centred cubic platinum metal.

The electron diffraction pattern of the Pt is seen as spots in Fig. 7a, which demonstrates that the sizes of Pt particles formed on the conventionally synthesized poly(*o*-phenylenediamine) polymer are large.

3.3. Evaluation of methanol oxidation activity of GR/Naf/Al₂O₃/PoPD_{Temp}-Pt nanotube and GR/Naf/Al₂O₃/PoPD_{Conv}-Pt electrodes

The cyclic voltammogram of Pt–poly(*o*-phenylenediamine) in the presence of in 1 M H₂SO₄ after the removal of the template is shown in Fig. 8a. A broad peak at –0.2 V in the forward scan was observed, due to the ionization of hydrogen on Pt. The CV for the Pt–poly(*o*-phenylenediamine) in 1 M H₂SO₄/1 M CH₃OH after the dissolution of the template is shown in Fig. 8b.

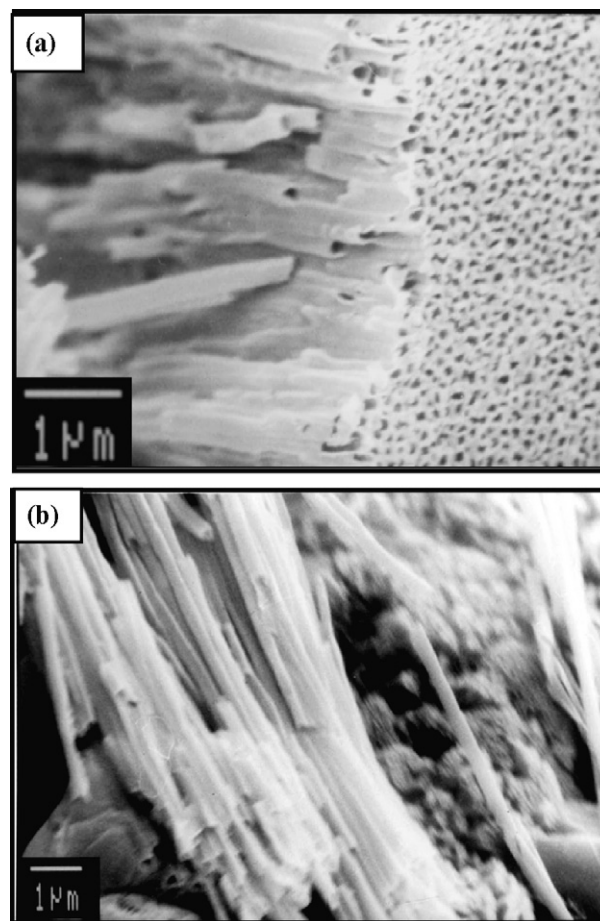


Fig. 5. SEM images of template-synthesized PoPD polymer nanotubes.

The methanol oxidation is clearly evident from the CV with a maximum current density of 84 mA cm^{–2}. Another interesting feature of the CV is that as the applied potential increases, the methanol oxidation current density also increases without peaking at any particular potential value (in the potential range studied). In the present investigation, the potential was scanned between –0.2 and +1.0 V versus Ag/AgCl. Though, there is no peak current observed in the cyclic voltammogram for Pt incorporated template-synthesized poly(*o*-phenylenediamine) nanotube electrode, the anodic peak current observed was taken and the values are normalized per unit area (mA cm^{–2}). The difference between the forward and the reverse current was also found to be very low, which might suggest the better tolerance of the electrode towards the strongly adsorbed intermediates. It was also reported that poisoning effect was lower on the Pt dispersed on the poly(*o*-phenylenediamine) than the bulk Pt electrodes [28].

Fig. 9 shows the cyclic voltammogram of GR/Naf/PoPD_{Conv}/Pt in 1 M H₂SO₄ and 1 M CH₃OH. It is clear from the voltammogram that the onset of methanol oxidation starts around +0.2 V in the forward scan and peaks at 0.7 V with a peak current density of 13.3 mA cm^{–2}, the reverse scan shows the oxidation peak at 0.45 V with a peak current density of 6 mA cm^{–2}. Based on the charge deposited for the polymerization, the thick-

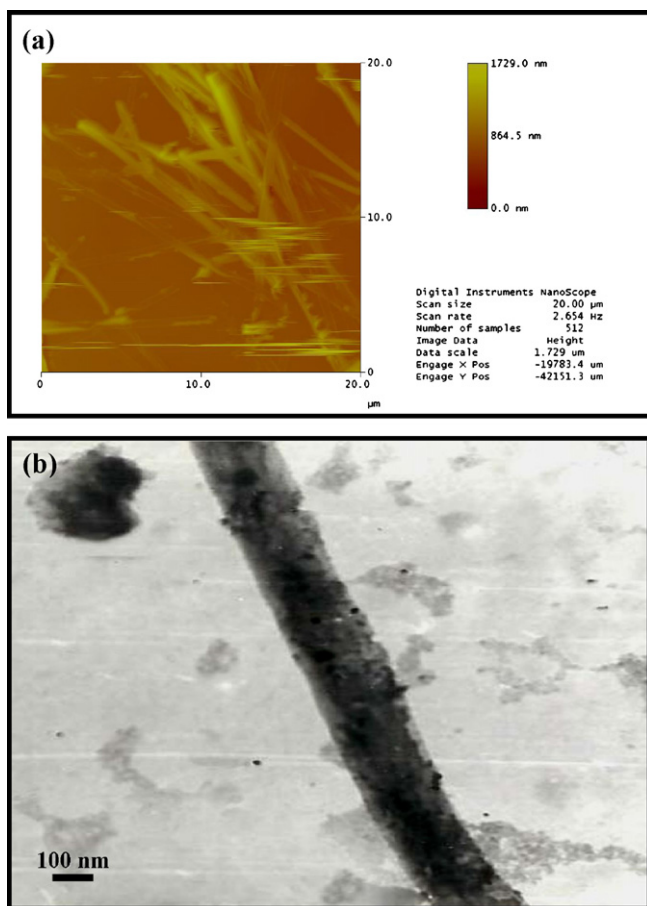


Fig. 6. (a) AFM images of template-synthesized PoPD polymer nanotubes on the silicon substrate and (b) TEM images of Pt deposited on template-synthesized PoPD polymer nanotubes.

ness of the polymer was found to be $0.6 \mu\text{m}$ and the loading of Pt was found to be $600 \mu\text{g cm}^{-2}$.

Since the Pt deposited on the conventionally synthesized poly(*o*-phenylenediamine) behaved like a bulk Pt, the curve in Fig. 9 was reminiscent of the Pt electrode [29]. But, though the catalyst is, Pt deposited on the poly(*o*-phenylenediamine) in both the cases, the curve in Fig. 8b for the templated electrode for methanol oxidation was different compared to the conventional electrode. The peak potential for methanol oxidation was not observed even up to $+0.8 \text{ V}$ versus Ag/AgCl electrode for the templated system. This is the main reason for the differences in the cyclic voltammogram between the two systems. This also probably reflects that the Pt loaded on the templated system was more resistant for oxide formation than the Pt loaded on the conventional poly(*o*-phenylenediamine) electrode. It is well known that Pt forms platinum oxide in aqueous solutions. It is normally observed that a Pt surface at $+0.8 \text{ V}$ versus Ag/AgCl should be largely oxidized [30,31] and in the present study with the Pt loaded on the conventionally synthesized poly(*o*-phenylenediamine), the same behavior was observed and that was one of the reasons for the decrease in activity of methanol oxidation (Fig. 9) beyond 0.7 V versus Ag/AgCl. In the case of templated system, it appears that the Pt particles in the templated nanotubes was comparatively more resistant for the Pt oxide for-

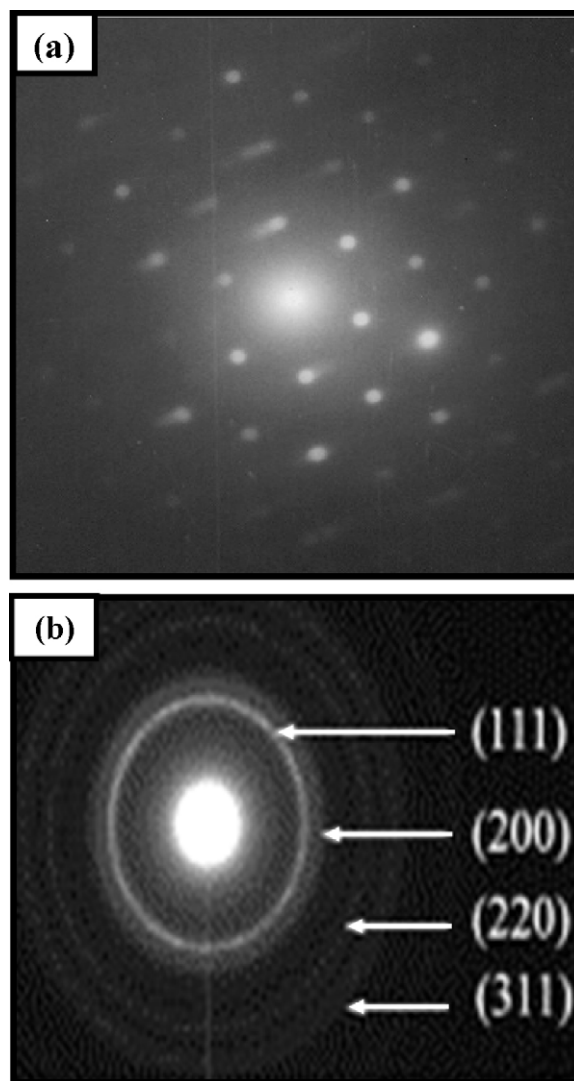


Fig. 7. Electron diffraction pattern of Pt nanoparticles on (a) conventionally synthesized PoPD polymer and (b) Pt nanoparticles template-synthesized PoPD polymer nanotubes.

mation, and this might be one of the reasons for the continuous increase in activity (Fig. 8b) even beyond 0.7 V versus Ag/AgCl electrode.

The activity of methanol oxidation evaluated for Pt incorporated template-synthesized poly(*o*-phenylenediamine) and Pt deposited on conventionally synthesized poly(*o*-phenylenediamine) from the cyclic voltammograms are tabulated in Table 1.

3.4. Effect of Pt loading on poly(*o*-phenylenediamine) nanotubes on the performance of methanol oxidation

Fig. 10 shows the plot of variation of performance of methanol oxidation current with Pt loading on conventionally synthesized poly(*o*-phenylenediamine) polymer and template-synthesized poly(*o*-phenylenediamine) polymer nanotubes. It is evident from the plot, as the loading increases there is an increase in the activity (84 mA cm^{-2}) of methanol oxidation up

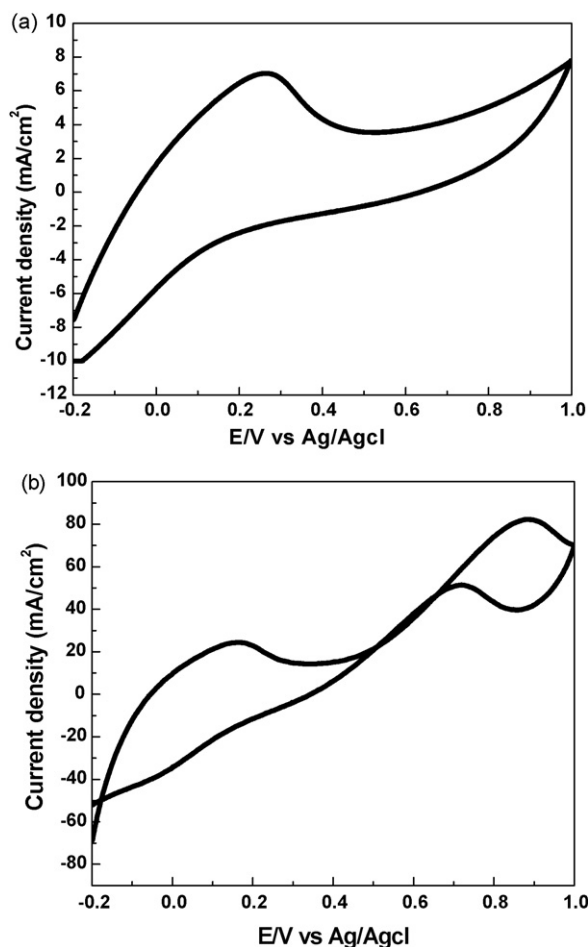


Fig. 8. Cyclic voltammograms of Pt incorporated template-based poly(*o*-phenylenediamine) (GR/Naf/Al₂O₃/PoPD_{Temp}-Pt) electrode (after the removal of template): (a) 1 M H₂SO₄ and (b) 1 M H₂SO₄/1 M CH₃OH. Scan rate 50 mV s⁻¹.

to a loading of 600 μg cm⁻². This clearly reveals that the nanotube morphology of the poly(*o*-phenylenediamine) polymer helps in the fine dispersion of the Pt particles inside the poly(*o*-phenylenediamine) matrix. As platinum loading increases the catalytic activity increases for the template-synthesized poly(*o*-phenylenediamine) polymer nanotubes. This is due to the nanotubular morphology of the polymer which can load platinum to a higher extent and at maximum loading, there is no further increase in the catalytic activity. But as the loading increases, there is no much increase in the catalytic activity for the conventionally synthesized poly(*o*-phenylenediamine) polymer electrode, probably due to the agglomeration of the

Table 1
Comparison of activity of methanol oxidation between GR/Naf/PoPD_{Temp}-Pt and GR/Naf/PoPD_{Conv}/Pt electrodes

Serial no.	Electrode	Onset potential (V)	Activity ^a			
			Forward sweep		Reverse sweep	
			<i>I</i> (mA cm ⁻²)	<i>E</i> (mV)	<i>I</i> (mA cm ⁻²)	<i>E</i> (mV)
1	GR/Naf/PoPD _{Temp} -Pt	+0.37	84	0.82	–	–
2	GR/Naf/PoPD _{Conv} -Pt	+0.2	13.3	0.70	6.0	0.45

^a Activity evaluated from cyclic voltammogram run in 1 M H₂SO₄/1 M CH₃OH.

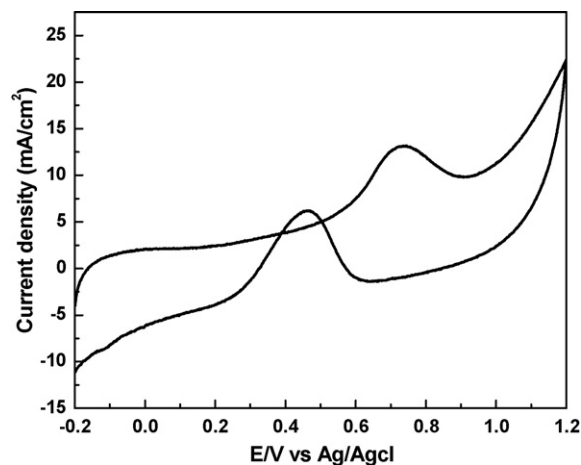


Fig. 9. Cyclic voltammograms of Pt incorporated conventional synthesized poly(*o*-phenylenediamine) (GR/Naf/Al₂O₃/PoPD_{Conv}-Pt) electrode (after the removal of template) in 1 M H₂SO₄/1 M CH₃OH. Scan rate 50 mV s⁻¹.

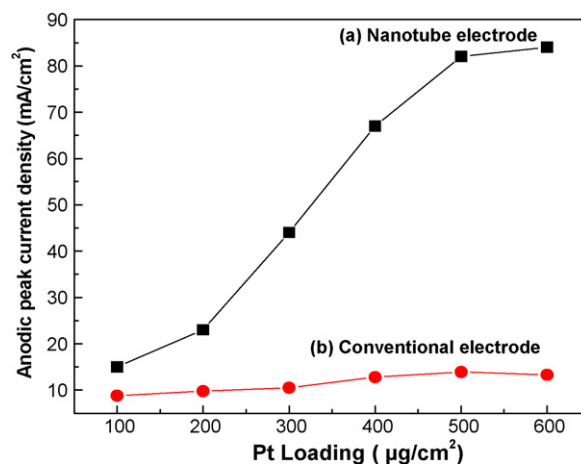


Fig. 10. Variation of anodic peak current density as a function of platinum loading on (a) nanotube and (b) conventional electrodes (current densities were evaluated from CV run in 0.5 M H₂SO₄/1 M CH₃OH at 50 mV s⁻¹).

catalytic particles, which restrict the usage of Pt particles for methanol oxidation. The charge used for the polymerization was 600 mC cm⁻².

3.5. Effect of methanol concentration

Fig. 11 shows the effect of methanol concentration on the anodic current of methanol oxidation for conventional and template-synthesized polymer nanotube electrodes. It is clearly

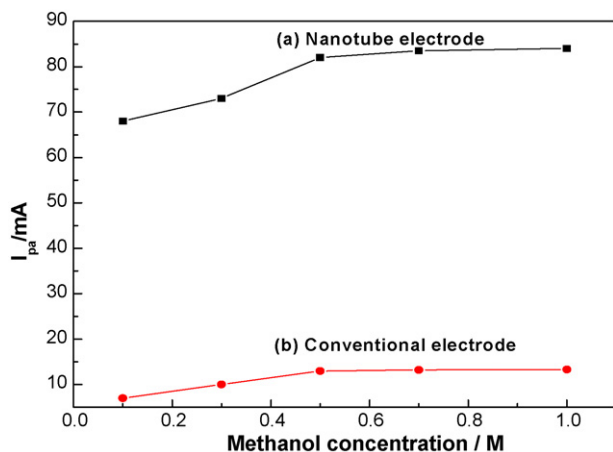


Fig. 11. Plot of anodic peak current of methanol oxidation as a function of methanol concentration in 0.5 M H_2SO_4 solution for (a) nanotube and (b) conventional electrodes.

observed that the anodic current increases with increasing methanol concentration and levels off at concentrations higher than 0.5 M at both conventional and nanotube electrodes. We assume that this effect may be due to the saturation of active sites on the surface of the electrode. In accordance with this result, the optimum concentration of methanol to obtain a higher current density may be considered about 0.5–1 M. As seen in Fig. 11 the largest current for a given concentration of methanol was observed on the GR/Naf/PoPD_{Temp}-Pt electrode in same experimental conditions.

3.6. Effect of temperature

The effect of temperature on the electro-oxidation of methanol was studied. It is found that the anodic current at two different electrodes affected by temperature is shown in Fig. 12. Current density generally increases with the rise in temperature indicating an increase in reaction kinetics. A linear increase in the peak currents with increasing temperature was observed for

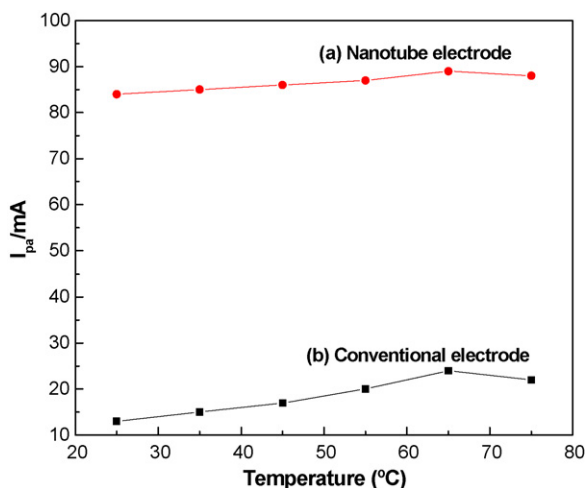


Fig. 12. Plot of anodic peak current oxidation as a function of temperature for (a) GR/Naf/PoPD_{Temp}-Pt and (b) GR/Naf/PoPD_{Conv}-Pt in 0.5 M H_2SO_4 /1.0 M CH_3OH .

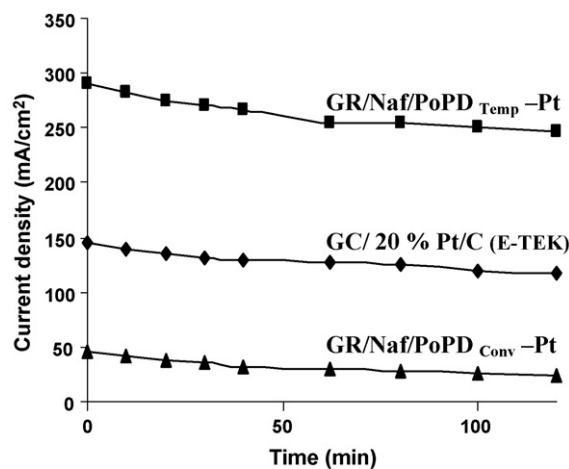


Fig. 13. Variation of current density with time in 1 M H_2SO_4 /1 M CH_3OH at +0.6 V vs. Ag/AgCl.

the conventional electrodes up to 65 °C, indicating an enhancement of the methanol oxidation rate with temperature and then the peak currents decrease. The next decrease can be attributed to the progressive evaporation of solution with increasing temperature. Considering that no azeotrope is formed in methanol water mixture, it is expected that a progressive decrease in peak current should appear during the temperature elevation, due to a loss in methanol concentration. However, a linear increase of the peak current is observed in practice at temperatures below 65 °C (the boiling point of methanol is 64.5 °C), which can be assigned to the acceleration of the electrode reaction kinetics proportionally to temperature increase. There is no much increase in current density as temperature increases for template-synthesized nanotube electrode. This may be due to the tubular morphology favouring easier transport of methanol to the catalytic sites.

3.7. Chronoamperometric response of GR/Naf/PoPD_{Temp}-Pt, GC/20 wt.%Pt/C (E-TEK) and GR/Naf/PoPD_{Conv}-Pt

Chronoamperometric experiments were carried out to observe the stability and possible poisoning of the catalysts under short-time continuous operation. Fig. 13 shows the evaluation of activity of GR/Naf/PoPD_{Temp}-Pt and GR/Naf/PoPD_{Conv}-Pt with respect to time at constant potential of +0.6 V. It is clear from Fig. 13 when the electrodes are compared under identical experimental conditions; the GR/Naf/PoPD_{Temp}-Pt shows a better activity and stability to the GR/Naf/PoPD_{Conv}-Pt, and GC/E-TEK 20% Pt/Vulcan XC72 carbon-nafion electrodes. GC/E-TEK 20% Pt/Vulcan XC72 carbon-nafion shows higher activity and stability compared to conventional GR/Naf/PoPD_{Conv}-Pt electrodes. The higher activity of the polymer nanotube-based electrodes demonstrates the better utilization of the catalyst. The increased utilization is mainly due to the tubular morphology of the polymer, which allows the particle to be highly dispersed, resulting in lower particle size. The lower activity of GR/Naf/PoPD_{Conv}-Pt and

GC/E-TEK 20% Pt/Vulcan XC72 carbon–nafion electrode might be due to the poor utilization of the platinum catalyst.

4. Conclusions

The electrochemical synthesis and characterization of conducting poly(*o*-phenylenediamine) nanotube and Pt incorporated nanotube by template method have been achieved. On the other hand, the SEM experiments show the dense, non-uniform and mat morphology of conventionally synthesized poly(*o*-phenylenediamine). The fine dispersion of Pt particles inside the nanotube was revealed from the electron diffraction image. The methanol oxidation activity of Pt incorporated template-synthesized poly(*o*-phenylenediamine) with a loading of $600 \mu\text{g cm}^{-2}$ was found to be nearly 13 times more active than Pt deposited on conventionally synthesized poly(*o*-phenylenediamine) with the same metal loading. It is revealed from the plot of current density versus the loading, that the Pt incorporated on template-synthesized poly(*o*-phenylenediamine) can accommodate more amount of Pt than conventionally synthesized poly(*o*-phenylenediamine). Excellent catalytic activity is observed for the electro-oxidation of methanol at the metal–polymer nanotube composite electrode. The highly dispersed platinum particles play a key role in the electrochemical behavior and catalytic activity, and the conducting polymer acts as an electron transfer matrix and a protective layer with a long time stability of electrode. The better utilization (by means of high activity at low Pt loading) and stability of the template-synthesized Pt incorporated poly(*o*-phenylenediamine) electrode have been demonstrated by comparing with Pt incorporated template-free conventionally synthesized poly(*o*-phenylenediamine) electrode. One of the major impediments to the commercialization of DMFC is the higher requirement of Pt catalyst. Increasing its utilization could considerably lower the Pt loading. The Pt incorporated template-synthesized polymeric nanotube on the graphite, not only increases the electronic–ionic contact, but also provides an easier electronic pathway between the electrode and the electrolyte, which increases the reactant accessibility to the catalytic sites.

The electro-catalytic activity of the nanotube-based electrode was compared to those of the conventionally synthesized poly(*o*-phenylenediamine) on graphite, using cyclic voltammetry. The Pt incorporated poly(*o*-phenylenediamine) nanotube electrode exhibited excellent catalytic activity and stability compared to the 20-wt.% Pt supported on the Vulcan XC 72R carbon and Pt supported on the conventional poly(*o*-phenylenediamine) electrode. The nanotube electrode showed excellent electro-catalytic

activity and stability for electro-oxidation of methanol. The electrode fabrication and the performance used in the present investigation is particularly attractive to adopt in the direct methanol fuel cells.

References

- [1] A.S. Arico, S. Srinivasan, V. Antonucci, *Fuel Cells* 1 (2001) 133.
- [2] A.J. Appleby, *J. Power Sources* 29 (1990) 3.
- [3] C.K. Dyer, *J. Power Sources* 106 (2002) 31.
- [4] M. Wang, D.J. Guo, H.L. Li, *J. Solid State Chem.* 178 (2005) 1996.
- [5] R.W. Lashway, *MRS Bull.* 30 (2005) 581.
- [6] M. Wang, *J. Power Sources* 112 (2002) 307.
- [7] J.R. Jewulski, Z.S. Rak, *Environ. Prot. Eng.* 32 (2006) 189.
- [8] S.G. Chalk, J.F. Miller, F.W. Wagner, *J. Power Sources* 86 (2000) 40.
- [9] T. Maiyalagan, B. Viswanathan, U.V. Varadaraju, *Electrochem. Commun.* 7 (2005) 905.
- [10] P.K. Shen, K.Y. Chen, A.C.C. Tseung, *J. Electrochem. Soc.* 142 (1995) L85.
- [11] T. Maiyalagan, B. Viswanathan, U.V. Varadaraju, *J. Nanosci. Nanotech.* 6 (2006) 2067.
- [12] J.M. Macak, P.J. Barczuk, H. Tsuchiya, M.Z. Nowakowska, A. Ghicov, M. Chojak, S. Bauer, S. Virtanen, P.J. Kulesza, P. Schmuki, *Electrochem. Commun.* 7 (2005) 1417.
- [13] J. Tian, G. Sun, L. Jiang, S. Yan, Q. Mao, Q. Xin, *Electrochem. Commun.* 9 (2007) 563.
- [14] M. Hapel, I. Kumarihamy, C.J. Zhong, *Electrochem. Commun.* 8 (2006) 1439.
- [15] C. Xu, P.K. Shen, *Chem. Commun.* 19 (2004) 2238.
- [16] C. Xu, P.K. Shen, X. Ji, R. Zeng, Y. Liu, *Electrochem. Commun.* 7 (2005) 1305.
- [17] Y. Bai, J. Wu, J. Xi, J. Wang, W. Zhu, L. Chen, X. Qiu, *Electrochem. Commun.* 7 (2005) 1087.
- [18] E. Auer, A. Freund, J. Pietsch, T. Tacke, *Appl. Catal. A: Gen.* 173 (1998) 259.
- [19] S.H. Joo, S.J. Choi, I. Oh, J. Kwak, Z. Liu, O. Terasaki, R. Ryoo, *Nature* 412 (2001) 169.
- [20] A.L. Dicks, *J. Power Sources* 156 (2006) 128.
- [21] L. Xiong, A. Manthiram, *Electrochim. Acta* 49 (2004) 4163.
- [22] B. Rajesh, K.R. Thampi, J.M. Bonard, N. Xanthopoulos, H.J. Mathieu, B. Viswanathan, *J. Power Sources* 141 (2005) 35.
- [23] D.J. Strike, N.F. De Rooij, M. Koudelka-Hep, M. Ulmann, J. Augustynski, *J. Appl. Electrochem.* 22 (1992) 922.
- [24] S.M. Golabi, A. Nozad, *J. Electroanal. Chem.* 521 (2002) 161.
- [25] T. Ohsaka, T. Watanabe, F. Kitamura, N. Oyama, K. Tokuda, *Chem. Commun.* 16 (1991) 1072.
- [26] Y.J. Li, R. Lenigk, X.Z. Wu, B. Gruendig, S.J. Dong, J. Shao, R. Renneberg, *Electroanalysis* 10 (1998) 671.
- [27] J. Premkumar, R. Ramaraj, *J. Appl. Electrochem.* 26 (1996) 763.
- [28] P. Santhosh, A. Gopalan, T. Vasudevan, K.P. Lee, *Appl. Surf. Sci.* 252 (2006) 7964.
- [29] K. Yamamoto, D.M. Kolb, R. Kotz, G. Lehmpfuhl, *J. Electroanal. Chem.* 96 (1979) 233.
- [30] D.S. Austin, J.A. Polta, T.Z. Polta, A.P.-C. Tang, T.D. Cabelka, D.C. Johnson, *J. Electroanal. Chem.* 25 (1984) 227.
- [31] S. Trasatti, O.A. Petrii, *Pure Appl. Chem.* 63 (1991) 711.